Research Square

Preprints are preliminary reports that have not undergone peer review.
They should not be considered conclusive, used to inform clinical practice,
or referenced by the media as validated information.

Historical demography of the dung beetle Canthon cyanellus LeConte, 1859: A neotropical species complex

Janet Nolasco-Soto

janet.nolasco@inecol.mx

INECOL: Instituto de Ecologia https://orcid.org/0000-0002-5979-6598

Jorge Arturo González-Astorga

INECOL: Instituto de Ecologia

Mario Enrique Favila

INECOL: Instituto de Ecologia

Jorge Ari Noriega

Universidad El Bosque

Alejandro Espinosa de los Monteros

INECOL: Instituto de Ecologia

Research Article

Keywords: Ancestral area, Colombia, Mexico, Pleistocene, Scarabaeinae, South America

Posted Date: July 24th, 2026

DOI: https://doi.org/10.21203/rs.3.rs-10386000/v1

License: This work is licensed under a Creative Commons Attribution 4.0 International License.
Read Full License

Historical demography of the dung beetle *Canthon cyanellus* LeConte, 1859: A neotropical species complex.

Janet Nolasco-Soto [1], Jorge González Astorga [1], Mario E. Favila [2], Jorge Ari Noriega [3], Alejandro Espinosa de los Monteros [1, *]

[1] Instituto de Ecología, A.C. Red de Biología Evolutiva, Xalapa, Veracruz, México.

[2] Instituto de Ecología, A.C. Red de Ecoetología, Xalapa, Veracruz, México.

[3] Universidad El Bosque, Facultad de Ingeniería, Grupo de Agua, Salud y Ambiente, Bogotá, Colombia.

*Corresponding author. E-mail: alejandro.espinosa@inecol.mx

Janet Nolasco-Soto [1], janet.nolasco@inecol.mx, https://orcid.org/0000-0002-5979-6598

Jorge González Astorga [1], jorge.gonzalez@inecol.mx, https://orcid.org/0000-0003-4755-8493

Mario E. Favila [2], mario.favila@inecol.mx, https://orcid.org/0000-0002-2737-9327

Jorge Ari Noriega [3], jnorieg@hotmail.com, https://orcid.org/0000-0003-1760-7020

Alejandro Espinosa de los Monteros [1, *], alejandro.espinosa@inecol.mx, https://orcid.org/0000-0002-7742-5977

Section: Systematics, Morphology and Physiology

Abstract

The role of geological and climatic events in driving intraspecific diversification in widely distributed insects in the Neotropic has been understudied. We investigated the genealogic relationships within and among populations of the dung beetle *Canthon cyanellus* from Mexico and Colombia using nuclear (*ITS2*) and mitochondrial (*16S*, *COI*) genetic markers to determine how past climatic fluctuations and geological events have shaped their demography and diversification. Our results revealed significant genetic variation across the sampled regions. The mtDNA region was the most informative, showing a gradient in genetic diversity. Analyses of all three markers indicated a historical demographic dynamic characterized by population expansions during interglacial and interstadial periods. Mainly, during the Pleistocene the populations of this species have diverged into seven clades in Mexico and two in Colombia. The genetic structure is consistent with a pattern of historical isolation by distance. In Colombia, the recovered clades agree with variation in color, and the genetic distinctiveness suggests that those clades might represent cryptic species. Pleistocene climatic changes, coupled with geological events such as the Andean uplift, were significant drivers of population divergence. The divergence between the Mexican and Colombian populations (ca. 2.81 Myr) coincides with the early formation of the Isthmus of Panama. This temporal correlation concurs with the hypothesis of a dispersal pathway from South America to North America.

Keywords: Ancestral area, Colombia, Mexico, Pleistocene, Scarabaeinae, South America.

Introduction

The Neotropic constitute one of the biogeographic regions with the greatest global biodiversity. Here, geological (e.g., the rise of the Andes) and climatic events (e.g., Pleistocene climate change) have promoted the emergence of biological barriers and corridors, influencing speciation and the dispersal pattern of the biota (Hoorn et al. 2010; Rull 2011; Fonseca et al. 2023). Perhaps, one of the most important Cenozoic events for Neotropical biogeography is the formation of the Isthmus of Panama (ca. 2.8 Myr), which allowed the Great American Biotic Interchange between previously isolated continental masses (O'Dea et al. 2016). Several studies (e.g., Cody et al. 2010; Smith et al. 2012; Bacon et al. 2016), have evaluated how such biological and geological events have impacted diversification mechanisms, and modified the biotic assemblage between North and South America. However, studies focused on arthropods, particularly insects, are still limited (butterflies: Arias et al. 2014; ants: Winston et al. 2017; Mendoza-Ramírez et al. 2018; Muñoz-Valencia et al. 2022; termites: Gergonne et al. 2023; beetles: Huang 2016; Chani-Posse et al. 2024; spiders: Salgado-Roa et al. 2024).

The origin of Dung beetles (Coleoptera: Scarabaeinae) is dated to the Early Cretaceous (115–130 Myr; Gunter et al. 2016), and their distribution may reflect recent geological events, exhibiting high dispersal capacity over short and medium distances (Vaz-de-Mello and Cupello 2018). The Mexican Transition Zone harbors species phylogenetically related to South American taxa, suggesting a shared evolutionary history (Halffter 1964, 1974, 1976). Within this group, the genus *Canthon* Hoffmannsegg, 1817 (Deltochilini Lacordaire, 1856) — comprising approximately 230 species and subspecies (Schoolmeesters 2026) — is endemic to the New World (from Canada to Argentina; Halffter and Martinez 1977). Some studies based on the distribution patterns of cenocrons suggest that *Canthon* and related genera originated in northern South America. Subsequently, they dispersed into Central and North America through events

facilitated by the geological dynamics of the Isthmus of Panama (Kohlmann and Halffter 1990; Halffter and Morrone 2017; Morrone 2020). Two major dispersal events have been identified: 1) during or before the Miocene, involving species of the subgenus *Canthon* (e.g., *pilularius*, *humectus*, *obliquus*, *imitator*) and *Boreocanthon*, as well as the genus *Melanocanthon* (Kohlmann and Halffter 1990); and 2) during the Plio-Pleistocene, corresponding to the species *Canthon cyanellus* LeConte, 1859 (Nolasco-Soto et al. 2017) and *Canthon indigaceus* LeConte, 1866 (Moctezuma et al. 2025). These species dispersed northward through the lowlands of the Pacific and Gulf of Mexico slopes without colonizing the Mexican mountain systems. This distribution corresponds to the typical Neotropical pattern, which is associated with tropical dry forests, cloud forests, and tropical forests at altitudes from sea level to 2000 m (Halffter and Morrone 2017). More recent dispersal events have occurred ca. 10,000 years ago. These were related to the expansion of tropical forests (e.g., *C.* (*Glaphyrocanthon*) *subhyalinus* Harold, 1867, *C.* (*Glaphyrocanthon*) *euryscelis* Bates, 1887, and *C.* (*Glaphyrocanthon*) *angustatus* Harold, 1867).

The taxonomic delimitation of *C. cyanellus* is among the most complex within the genus *Canthon*, owing to morphological variability among individuals from different populations and the pronounced polychromatism across its distribution (Solís and Kohlmann 2002). For Colombia, Schmidt (1922) described *Canthon sallei* var. *triangulatus*, which features a dark, triangular spot on the pronotum, accompanied by lateral spots that either do not join or may be absent. *Canthon sallei* var. *gutticollis* Schmidt, 1922, has a predominantly black coloration, with the pronotum having slight green reflections and small orange spots, as well as elytra with an orange spot (Fig. 1). Halffter (1961) pointed out that the varieties recognized by Schmidt should be accepted until a detailed study of Central and South American material is conducted that can designate them in the taxonomic category of subspecies. Even so, Halffter (1961) recognized three subspecies: 1) *C. c. cyanellus* LeConte, 1859; 2) *C. c. violetae* Halffter, 1961; and 3) *C. c.*

sallei Harold, 1863 (Fig. 1). Subsequently, Martínez (1988) described *C. c. havranekae* Martínez, 1988 for Venezuela, with coloration similar to *C. c. sallei*.

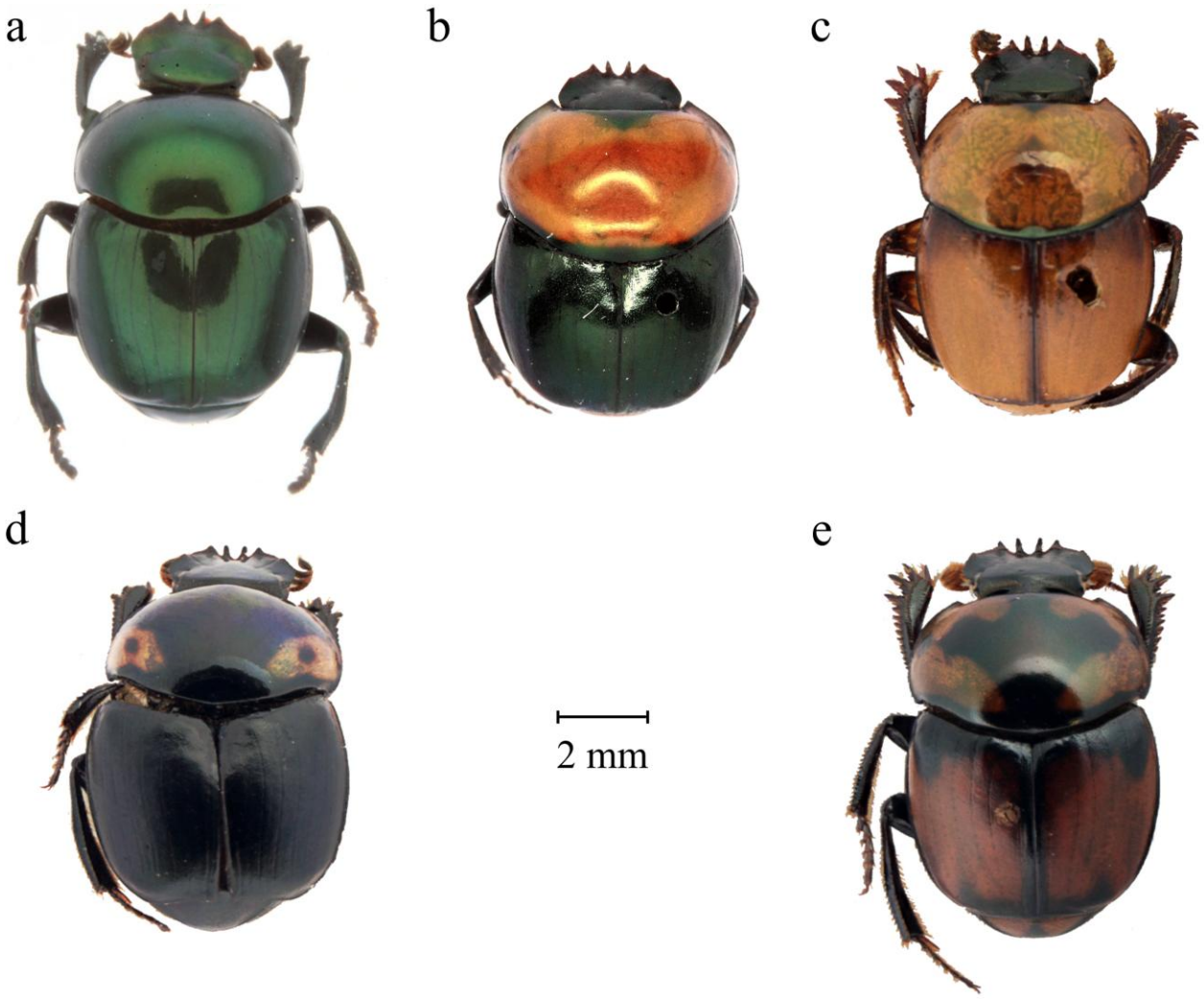


Fig. 1 Subspecies of *Canthon cyanellus*: a *C. c. cyanellus*. b *C. c. violetae.* c *C. c. sallei*. Varieties according to Schmidt, 1922: d *C. sallei* var. *guticollis.* e *C. sallei* var. *triangulatus*

Nolasco-Soto et al. (2017, 2020) focusing mainly on populations of *C. cyanellus* from Mexico concluded that: 1) there is genetic and spatial structure recovering at least seven lineages that diversified during the Pleistocene (similar to that observed in other beetle species Reyes et al.

2023, and grasshoppers Sanabria-Urbán et al. 2025); 2) geographic isolation has promoted a more significant genetic structure than the morphological one (e.g., aedeagus); 3) limited historical gene flow has favored isolation by distance and the rising of local haplotypes; 4) processes like geological events (e.g., volcanism), Pleistocene climatic fluctuations, cycles of forest contraction and expansion (Mush 2002; Ferrari et al. 2005; Capra et al. 2013) could be associated to cladogenesis; 5) demographic expansion has taken place during the Pleistocene; and 6) chromatic variation does not constitute a valid character for taxonomic delimitation or inference of speciation processes (similar to what has been proposed for other scarabaeines Maldaner et al. 2019; Cupello et al. 2021).

Analyzing the population dynamics (e.g., expansions, bottlenecks, contractions) of widely distributed Neotropical species, such as *C. cyanellus*, contributes to understanding diversification processes and the historical factors that drive them. Furthermore, these studies are particularly relevant in taxonomically complex groups, where the integration of population genetic data allows for more precise species delimitation (Cupello et al. 2023). With this in mind, the objective of this study is to evaluate whether climatic fluctuations and geological events have influenced the demography and diversification of *C. cyanellus*, and how these environmental processes have modified its evolutionary history, genetic diversity, and current distribution. Specifically, we will attempt to answer the following questions: 1) Does genetic diversity increase consistently along a latitudinal gradient? 2) Is there significant population genetic structure across geographic regions? 3) When did the key cladogenesis events occur? 4) What is the populations' historical demography? And 5) Is the biogeographical scenario consistent with the contemporary distribution of *C. cyanellus*?

Material and methods

Sampling, DNA extraction, and sequencing

This study is an ongoing effort attempting to understand the evolutionary history and taxonomic delimitation of *C. cyanellus*. Therefore, we have taken data previously used from fourteen sites located in the Sierra Madre Oriental, the coast of the Gulf of Mexico, the Pacific slope of Mexico, and Tolima in Colombia that have been used for phylogeographical analyses (Nolasco-Soto et al. 2017 - Access Numbers: from KX807611 to KX807722; Nolasco-Soto et al. 2020 - Access Numbers: *16S*, from MK863451 to MK863505; *ITS2*, from MK873027 to MK873079; and *COI*, from MK882624 to MK882657). This sampling scheme has been complemented with new samples from Ocozocoautla, Chiapas, Mexico, and eight new collecting sites in Colombia (Fig. 2). We have included most of the chromatic variation described for the species (Table 1, Fig. S1). A total of 46 new specimens were collected using pitfall traps baited with a mixture of human and pig excrement. In the field, beetles were stored in ethanol, and frozen at −20°C once they arrived at the laboratory. Two hind legs of each beetle were macerated for DNA extraction following the DNeasy Blood & Tissue kit protocol (QIAGEN).

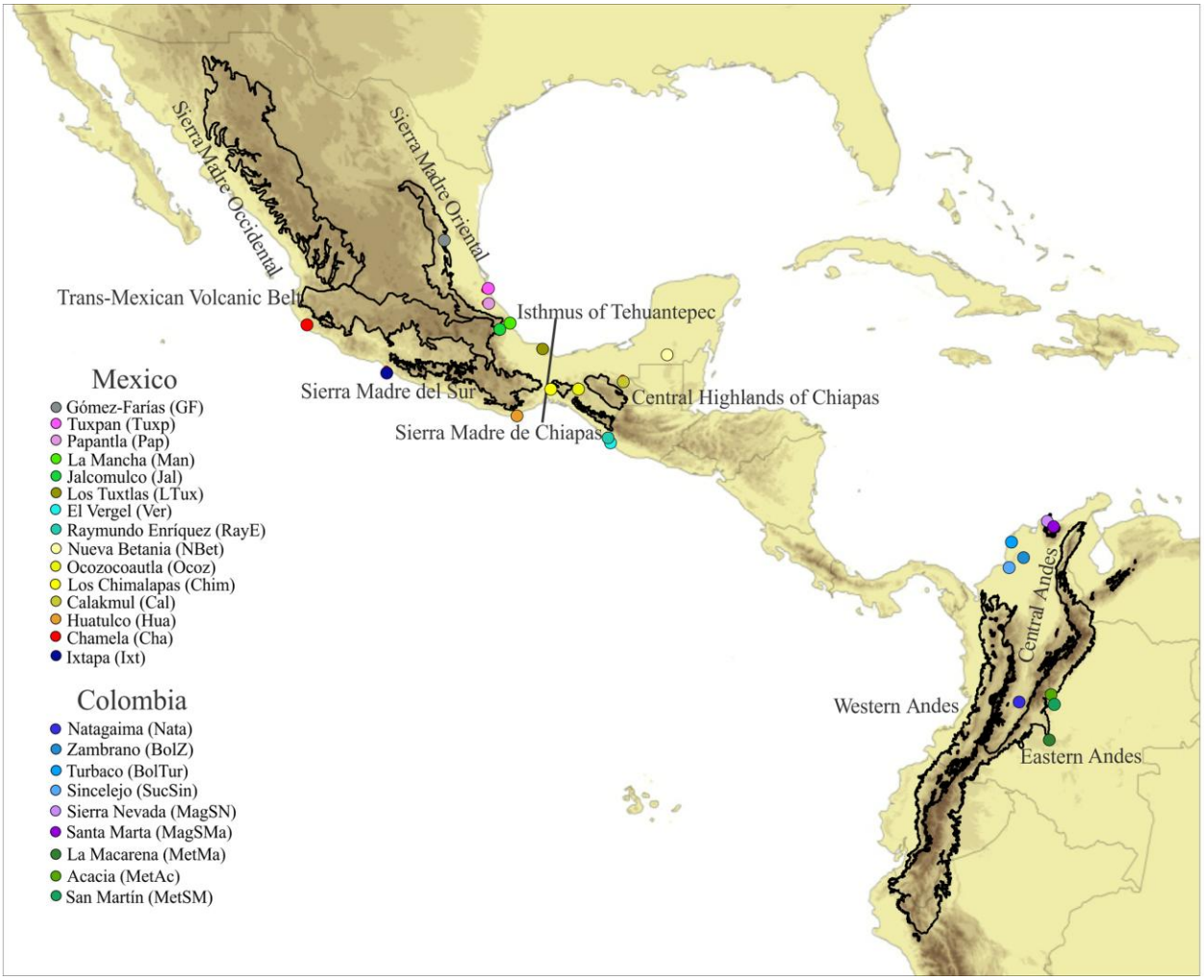


Fig. 2 Distribution of *Canthon cyanellus*. The Mexican Mountain systems and the Andes Mountain ranges in Colombia are highlighted with black contour lines

Table 1 *Canthon cyanellus* sampling locations. ID = locality identification code; *N is the number of individuals sequenced in this study, and Elev = elevation meters above sea level

Country	State	Locality	ID	N	Lat., Long.	Elev	Vegetation
Mexico	Tamaulipas	Gómez-Farias	GF	10	23.048, -99.143	379	Semi-deciduous tropical
Mexico	Veracruz	Tuxpan	Tuxp	10	20.954, -97.466	52	Rain-fed permanent
Mexico	Veracruz	Papantla	Pap	6	20.417, -97.450	200	Secondary herbaceous vegetation derived from evergreen tropical forest

Mexico	Veracruz	La Mancha	Man	10	19.569, -96.409	194	Rain-fed annual and semi-permanent agriculture
Mexico	Veracruz	Jalcomulco	Jal	10	19.329, -96.747	370	Rain-fed annual and permanent agriculture
Mexico	Veracruz	Los Tuxtlas	LTux	10	18.583, -95.067	120	Secondary vegetation derived from evergreen tropical forest and grasslands
Mexico	Chiapas	Raymundo-Enriquez	RayE	11	14.864, -92.301	99	Rain-fed permanent agriculture
Mexico	Chiapas	El Vergel	Ver	10	14.703, -92.267	22	Rain-fed annual agriculture
Mexico	Chiapas	Nueva Betania	NBet	10	17.282, -91.647	140	High evergreen forest
México	Chiapas	Ocozocoautla	Ocoz	10*	16.944, -93.530	937	Grasslands
Mexico	Oaxaca	Huatulco	Hua	10	15.780, -96.090	30	Mid-stature deciduous tropical forest
Mexico	Oaxaca	Los Chimalapas	Chim	10	16.912, -94.669	212	Grasslands
Mexico	Campeche	Calakmul	Cal	9	18.330, -89.823	225	Medium semi-evergreen
Mexico	Jalisco	Chamela	Cha	10	19.499, -105.023	90	Low deciduous tropical
Mexico	Guerrero	Ixtapa	Ixt	12	17.658, -101.575	120	Low deciduous tropical
Colombia	Tolima	Natagaima	Nata	14	3.648, -74.999	328	Tropical dry forest
Colombia	Bolívar	Zambrano	BolZ	9*	9.677, -74.837	20	Tropical dry forest
Colombia	Bolívar	Turbaco	BolTur	5*	10.354, -75.428	140	Tropical humid forest
Colombia	Magdalena	Sierra Nevada	MagSN	1*	11.137, -74.111	788	Tropical dry mountain
Colombia	Magdalena	Santa Marta	MagSM	2*	11.298, -73.927	50	Tropical rainforest
Colombia	Sucre	Sincelejo	SuSin	6*	9.318, -75.387	180	Tropical dry forest remnant
Colombia	Meta	La Macarena	MetMa	7*	2.139, -73.767	247	Tropical humid forest
Colombia	Meta	Acacias	MetAc	1*	3.957, -73.748	532	Gallery forest fragments
Colombia	Meta	San Martín	MetSM	5*	3.614, -73.642	361	Gallery forest fragments

The samples were sequenced for two mitochondrial markers (*16S* and *COI* mtDNA) and for the *ITS2* nuclear marker (nDNA; Table S1). All PCRs were performed in a 25 µL reaction volume using 2 µL of the DNA extraction, 4 µL of 5X buffer, 2 µL of $MgCl_2$ (25 mM), 2.5 µL of dNTPs (2 mM), 0.25 µL of bovine serum albumin (10 mg/mL), 0.8 µL of each primer (10 µM), 0.1 µL of Taq polymerase (5 U/µL), and 12.55 µL of ddH2O. The thermocycling profile included an initial denaturation step at 94°C for 180 seconds, followed by 30 cycles of denaturation at 94°C for 60 seconds, annealing at 48°C for 30 seconds, and extension at 70°C for 90 seconds, finishing with a final extension at 72°C for 180 seconds. Variations of this protocol were applied

for difficult samples. PCR products were subjected to electrophoresis in 1% TAE agarose for visualization. Successful reactions were purified using the Wizard® SV Gel and PCR Clean-Up System (PROMEGA) and sent to Macrogen for sequencing. Electropherograms were edited with the software SEQUENCHER v.5 (Gene Codes Corp., Ann Arbor, MI, USA) and aligned using MEGA X v10.2.2 (Kumar et al. 2018). The final alignment was refined manually.

Genetic diversity

Due to the widespread distribution of *C. cyanellus*, three geographic regions were defined: South America (SA), Mesoamerica (MeA), and North America (NA). This division is based on biogeographic criteria, reflecting differences in evolutionary history, ecological composition, and potential barriers to dispersal. This allows for the exploration of spatial patterns of genetic diversity and the evaluation of potential regional differentiation processes. For each locus, nucleotide (π) and haplotype (Hd) diversity (Nei and Li 1979) were estimated using DnaSP v6.12.03 (Rozas et al. 2017). To estimate whether there are significant differences in genetic diversity (π and Hd) between different geographical regions, ANOVAs were carried out by locus and followed by a Tukey test (HSD) using XLSTAT 2024.3. To assess whether there is a latitudinal pattern in genetic variation, a linear regression analysis was performed between the genetic diversity parameters and the geographic latitude of each population for each locus using XLSTAT 2024.3.

Genetic structure

Haplotype networks were constructed for each locus using the TCS algorithm in PopART (Leigh and Bryant 2015). An AMOVA was performed for each locus among the three designated geographic regions (i.e., SA, MeA, and NA) using Arlequin v3.5 software (Excoffier and Lischer

2010). To identify genetically congruent geographic regions, the fixation index (F_{CT}, Excoffier et al. 1992) was calculated with the computer program SAMOVA v1 (Dupanloup et al. 2002). The SAMOVA was performed on the combined dataset (*ITS2* + *16S* + *COI*) and by locus, allowing us to determine the number of groups that are statistically significant and consistent with their geographic distribution. Finally, to test the isolation by distance between populations, a Mantel test was carried out between the pair-wise population geographic distances and the corresponding F_{ST} values; this analysis was performed using Excel.

Genealogy of *Canthon cyanellus*

Genealogy was inferred from the total dataset (*ITS2* + *16S* + *COI*). Outgroup homologous sequences were downloaded from the GenBank database (Table S2). *ITS2* sequences were not available in GenBank for any of the outgroup taxa; thus, we sequenced this marker for *C. indigaceus* and *C. occidentalis*.

Bayesian inference analysis was performed using MrBayes v.3.2.6 (Ronquist et al. 2012), accessed through the CIPRES portal (Miller et al. 2010). The nucleotide substitution model for each locus was selected using the Akaike Information Criterion in jModelTest v.2.1.8 (Darriba et al. 2012). The three nucleotide partitions were set as unlinked. Two parallel analyses were conducted, and Markov Chain Monte Carlo (MCMC) was run for 50 million generations. The program TRACER v.1.7.2 (Rambaut et al. 2018) was used to assess stationarity and effective sample sizes (ESS > 200). Trees and parameters were sampled every 1000 generations, and posterior probabilities (PP) were obtained from the majority-rule consensus tree after discarding the initial 25% of the sampled trees (Ronquist et al. 2012). The inferred tree was visualized using FigTree v.1.3.1 (Rambaut 2008).

Cladogenesis and historical demography

To date and infer cladogenetic events in the evolutionary history of *C. cyanellus*, we used the software BEAST v1.8.0 (Drummond et al. 2012). The Bayesian tree inferred was used as the tree prior. Divergence times were estimated using the 'relaxed clock' model. For dating the genealogy, we used the following nucleotide substitution rates: 2% s/s/My for *COI* (Papadopoulou et al. 2010), 1.2% for *16S* rRNA, and 0.85% for *ITS2* (Caccone et al. 1988). The nucleotide substitution models, as well as the parameters used as priors for each locus, were those indicated by jModelTest. The constant population size coalescent model was used for the tree model. MCMC analyses were run for 20 million generations, sampling trees and parameters every 1000 generations. Two independent runs were performed, each with one cold and three hot chains. The program TRACER v1.7.2 was used to assess MCMC stationarity, ESSs > 200, and posterior intervals encompassing the 95% highest posterior density. These analyses were repeated two times, and the resulting trees from each run were combined using LogCombiner v1.8.0, with a 25% burn-in. Nodes were evaluated for PP values > 0.8. To determine the historical demographic dynamics of the populations, a Bayesian skyline plot analysis was conducted using BEAST v1.8.0. The priors and molecular clock model used were identical to those applied in the coalescence analysis for node dating. Skyline plots were generated for the major lineages recovered.

Ancestral area, dispersal, and vicariance processes

To differentiate between potential dispersal and vicariance events in the evolutionary history of *C. cyanellus*, we performed a statistical dispersal-vicariance analysis (S-DIVA) using RASP v4.3 (Yu et al. 2020). Ancestral states for each node in the condensed tree were reconstructed using the

remaining 75% of trees (i.e., 39,996 trees after the 'burn-in' phase) generated in BEAST. For the ingroup, we used the three designated geographical regions.

Results

Genetic diversity

The alignment obtained from the three loci encompassed 2,202 base pairs (*ITS2* = 672 bp, *16S* = 767 bp, and *COI* = 763 bp). The number of haplotypes was 16 for *ITS2*, 52 for *16S*, and 97 for *COI*. New sequences were uploaded to GenBank (Table S2). Genetic diversity was lower for the nuclear *ITS2* than for the mitochondrial loci (*16S* and *COI*) (Table 2). The ANOVA for π revealed differences between loci ($p < 0.003$). A Tukey test showed differences only between *ITS2* and *COI* ($p < 0.011$). Similarly, ANOVA for Hd indicated differences between loci ($p < 0.0001$). The Tukey test revealed deviation between *16S* and *ITS2* ($p < 0.0001$) and between *16S* and *COI* ($p < 0.03$). The ANOVA for genetic diversity parameters by geographic region indicates differences for Hd in the *ITS2* locus ($p < 0.02$) but not for π ($p < 0.053$). Tukey's test revealed differences in Hd between MeA and SA ($p < 0.022$) (Table S3). The ANOVA for the genetic diversity parameters for the mitochondrial loci indicates differences among regions (*16S* π, $p < 0.001$; *16S* Hd, $p < 0.0001$; *COI* π, $p < 0.0001$; *COI* Hd, $p < 0.0001$). The Tukey's test showed differences for π between MeA and SA in both loci (*16S* π, $p < 0.001$; *COI* π, $p < 0.0001$). The Hd for *16S* and *COI* were different between MeA and SA ($p < 0.0001$); as well as between MeA and NA ($p = 0.011$) for the *COI* (Table S3).

Table 2 Molecular diversity indices for each locality and locus, including sample size (n), number of haplotypes (H), nucleotide diversity (π), and haplotype diversity (Hd)

Locality	ID	*ITS2*	*16S*	*COI*	*ITS2*	*16S*	*COI*	*ITS2*	*16S*	*COI*	*ITS2*	*16S*	*COI*
		n	n	n	H	H	H	π	π	π	Hd	Hd	Hd
North America	NA												
Gómez-Farias	GF	10	10	10	2	4	6	0.0005	0.0084	0.0249	0.3560	0.6440	0.8330
Tuxpan	Tuxp	10	10	8	1	5	4	0.0000	0.0015	0.0058	0.0000	0.8000	0.7500
Papantla	Pap	6	6	6	2	3	3	0.0009	0.0012	0.0054	0.6000	0.7330	0.6000
Mean								0.0005	0.0067	0.0200	0.3187	0.8340	0.8590
SD								0.0002	0.0013	0.0031	0.3017	0.0380	0.0550
Mesoamerica	MeA												
La Mancha	Man	10	10	10	1	4	10	0.0000	0.0012	0.0127	0.0000	0.7110	1.0000
Jalcomulco	Jal	10	10	10	2	6	10	0.0003	0.0020	0.0139	0.2000	0.8670	1.0000
Los Tuxtlas	LTux	10	10	10	2	6	6	0.0000	0.0034	0.0107	0.5333	0.8440	0.8890
Raymundo-Enriquez	RayE	11	11	11	3	5	9	0.0006	0.0016	0.0114	0.3450	0.7820	0.9640
El Vergel	Ver	10	10	10	2	5	9	0.0003	0.0015	0.0068	0.2000	0.7560	0.9780
Nueva Betania	NBet	10	10	6	1	3	4	0.0000	0.0028	0.0071	0.0000	0.5110	0.8000
Ocozocoautla	Ocoz	10	10	10	4	5	9	0.0013	0.0060	0.0206	0.5330	0.7560	0.9780
Huatulco	Hua	8	10	9	1	8	7	0.0000	0.0028	0.0030	0.0000	0.9560	0.9170
Los Chimalapas	Chim	10	10	2	2	6	2	0.0003	0.0106	0.0322	0.2000	0.7780	1.000
Calakmul	Cal	7	9	0	1	4	-	0.0000	0.0098	-	0.0000	0.6940	-
Chamela	Cha	10	10	10	1	4	4	0.0000	0.0011	0.0011	0.0000	0.5330	0.6440
Ixtapa	Ixt	12	12	12	2	4	8	0.0006	0.0014	0.0062	0.4090	0.6360	0.8940
Mean								0.0012	0.0109	0.0114	0.6210	0.9300	0.9900
SD								0.0001	0.0006	0.0088	0.0270	0.0110	0.0030
South America	SA												
Natagaima	Nata	14	14	14	2	1	4	0.0004	0.0000	0.0012	0.1430	0.0000	0.4950
Zambrano	BolZ	8	8	8	2	1	2	0.0006	0.0000	0.0007	0.4290	0.0000	0.2500
Turbaco	BolTur	1	5	1	1	2	1	0.0000	0.0001	0.0000	0.0000	0.4000	0.0000
Sierra Nevada	MagSN	1	1	1	1	1	1	0.0000	0.0000	0.0000	0.0000	0.0000	0.0000
Santa Marta	MagSMa	1	2	2	1	1	1	0.0000	0.0000	0.0000	0.0000	0.0000	0.0000
Sincelejo	SucSin	4	6	6	1	1	1	0.0000	0.0000	0.0000	0.0000	0.0000	0.0000
La Macarena	MetMa	7	7	1	2	4	1	0.0004	0.0016	0.0000	0.2860	0.7140	0.0000
Acacias	MetAc	0	1	1	0	1	1	-	0.0000	0.0000	-	0.0000	0.0000
San Martín	MetSM	3	5	5	1	3	5	0.0000	0.0013	0.0037	0.0000	0.7000	1.0000
Mean								0.0058	0.0047	0.0147	0.7400	0.4690	0.8100
SD								0.0008	0.0007	0.0028	0.0330	0.0800	0.0470

Global												
Mean	183	197	163	16	52	97	0.0061	0.0163	0.0401	0.8180	0.9340	0.9830
SD							0.0005	0.0005	0.0007	0.0170	0.0090	0.0040

The linear regressions between latitude and the genetic diversity were statistically significant for the mitochondrial loci, but not for the nuclear one (Table 3). For the mitochondrial markers, π for the *16S* changes with a positive rate of $2x10^{-4}$ as the latitude increases, whereas, for the *COI* π has a rate four times higher. Finally, latitude has a significant intermediate effect on Hd for both mitochondrial markers (Table 3, Fig. S2).

Table 3 Linear regression models for the relationship between latitude *vs.* π and Hd

Marker	Model	R^2	*P*
ITS2	$\pi = 6x10^{-6}Lat + 2x10^{-4}$	0.0097	0.6540
16S	$\pi = 2x10^{-4}Lat - 9x10^{-4}$	0.2185	0.0213
COI	$\pi = 8x10^{-4}Lat - 3.8x10^{-3}$	0.3178	0.0051
ITS2	$Hd = 7.2x10^{-3}Lat + 7.9x10^{-2}$	0.0414	0.3516
16S	$Hd = 3.1x10^{-2}Lat + 9.5x10^{-2}$	0.3253	0.0036
COI	$Hd = 7x10^{-2}Lat + 5x10^{-2}$	0.3657	0.0022

Genetic structure

The *ITS2* haplotype network consists of 16 haplotypes interconnected by 1 up to 6 mutational changes (Fig. S3). Three haplogroups are identified: Haplogroup I includes all populations from Mexico, and comprises 10 haplotypes; Haplogroup II consists of four haplotypes and includes all localities from northern Colombia, specifically those from the departments of Sucre, Magdalena, Bolívar, and Natagaima; and Haplogroup III encompasses all localities from the Meta department in Colombia. Geographically, the Eastern Andean Cordillera is separating Haplogroup III from

the other two haplogroups. The *16S* haplotype network consists of eight haplogroups with 52 haplotypes interconnected from 1 to 7 mutational changes (Fig. S4). Haplogroups II and III include all localities from Colombia. The other six haplogroups are identified in Mexico: Haplogroup I includes three localities from the southern Gulf of Mexico (i.e., Jal, Man, LTux; site ID is presented in Table 1), two localities from southern Chiapas (i.e., Ver and RayE), and four localities from southeastern Mexico (i.e., Ocoz, Chim, Cal, and NBet). The remaining haplogroups consist of samples from single populations (e.g., Hua in haplogroup IV, GF in haplogroup VI, and Ixt in haplogroup VII), except for haplogroup V, which includes all individuals from Tuxp and Pap, four individuals from GF, and one sample from LTux. Lastly, haplogroup VIII includes all individuals from the Cha locality and five individuals from Cal. In the *COI* haplotype network, nine haplogroups are identified, with 97 haplotypes interconnected from 1 to 23 mutations (Fig. S5).

The AMOVA showed that independently of the locus, most of the genetic variation occurs between geographic regions, rather than between populations within regions (Table 4). The population clusters inferred by the SAMOVA indicated that the optimal grouping was obtained at K = 10 (Table S4). Two groups were identified in Colombia (i.e., populations from the northern and central regions, and populations from the southern region of the Eastern Andes Mountain range), whereas the remaining eight clusters corresponded to populations in Mexico. SAMOVA by locus indicated similar population clusters with respect to the groupings obtained with the three loci, particularly among mtDNA markers for K = 10 (100% and 80% for *16S* and *COI*, respectively) (Table S5). The Mantel test revealed a positive correlation between geographic distance and F_{ST} independently of the locus, suggesting isolation by distance (Fig. 3).

Table 4 Analysis of molecular variance per locus. Geographic region = North America; Mesoamerica, and South America. BGR = between geographic regions. BPwGR = between populations within geographic regions. WP = within populations

Marker		df	SS	Est. var.	Var. (%)	
ITS2	BGR	2	347.124	3.435	72.16	F_{CT} = 0.722*
	BPwGR	20	181.771	1.148	24.11	F_{SC} = 0.866*
	WP	160	28.390	0.177	3.73	F_{ST} = 0.963*
	Total	182	557.284	4.760		
16S	BGR	2	500.387	4.261	52.79	F_{CT} = 0.528*
	BPwGR	21	470.695	2.630	32.59	F_{SC} = 0.690*
	WP	173	204.091	1.180	14.62	F_{ST} = 0.854*
	Total	196	1175.173	8.071		
COI	BGR	2	925.699	8.944	46.38	F_{CT} = 0.464*
	BPwGR	20	1048.810	7.236	37.53	F_{SC} = 0.700*
	WP	140	434.276	3.102	16.09	F_{ST} = 0.839*
	Total	162	2408.785	19.289		

*P < 0.0001

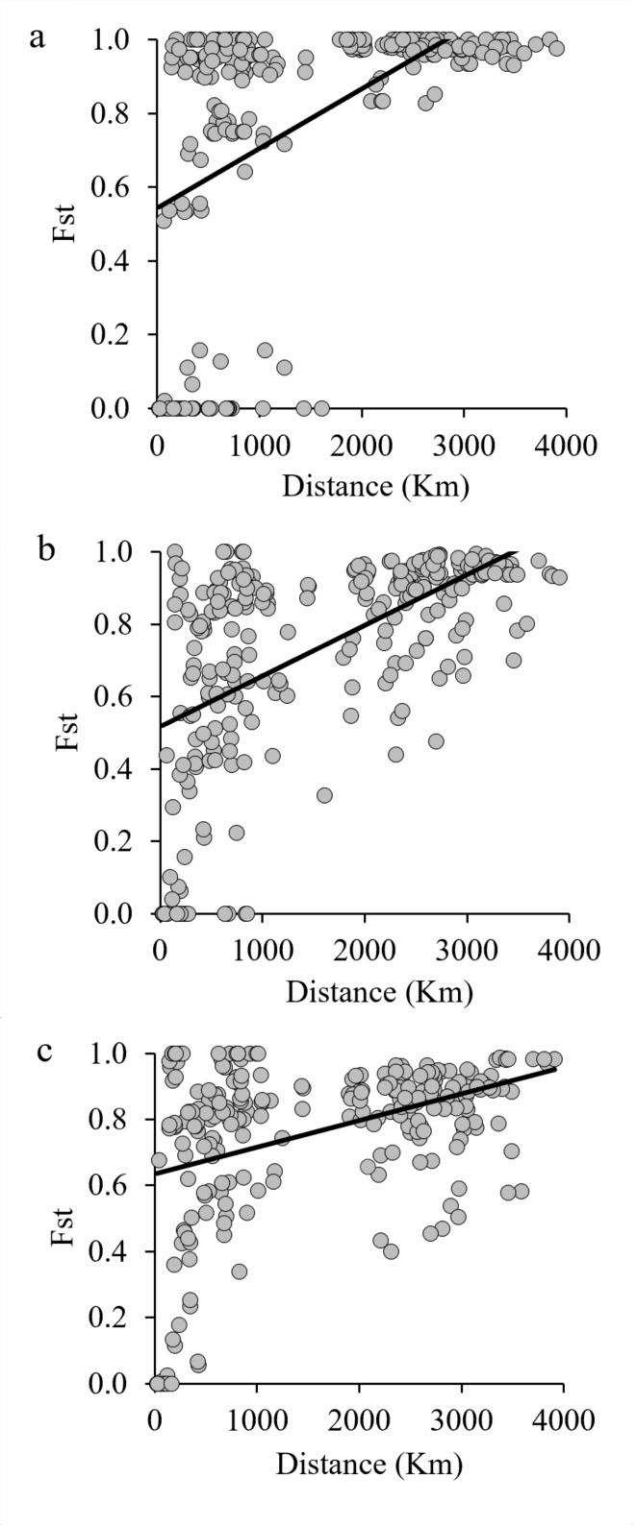


Fig. 3 Mantel test between geographic distance (Km) and F_{ST} by locus: a *ITS2* ($R^2 = 0.273$, $p < 0.0001$), b *16S* ($R^2 = 0.319$, $p < 0.0001$), and c *COI* ($R^2 = 0.156$, $p < 0.0001$)

Genealogy

The best-fit nucleotide substitution models and their specific parameters can be consulted in Table S6. The genealogy reconstructed from the combined dataset supported the monophyly of *C. cyanellus* (PP = 1) (Fig. S6). The first division in the genealogy separates the Mexican and the Colombian clades, which are well supported (PP = 1). Within the Colombian clade, two monophyletic groups were recovered. The first group includes all the localities from northern and central Colombia (PP = 1), while the second comprises all the localities south of the Andean Eastern Cordillera (PP = 1). Within the Mexican clade, five well-supported clades (PP = 1) are distinguished. One encompassing all individuals from the Hua locality in the South Pacific; a second clade, named here as "NGM", which contains four individuals from GF, all samples from the Pap and Tuxp, localities located north of the Transversal-Mexican Volcanic Belt. A third clade encompasses three subclades. The first includes all individuals from Ixt, which is sister to six individuals from GF; being those two sisters to a third subclade ChaCal encompassing all individuals from the locality Chamela, and five individuals from Calakmul. The remaining clades (SGM, SPS, and SEM) have low PP values (i.e., 0.75, 0.76, and 0.73, respectively).

Diversification times and demographic history

The chronogram inferred from the combined dataset (Fig. 4) indicates that the Colombian and Mexican clades of *C. cyanellus* diverged during the Miocene, approximately 2.81 Myr ago. Subsequent diversification events that gave rise to the main lineages of *C. cyanellus* in Mesoamerica, North America, and South America occurred during the Pleistocene, within a time range from 1.80 to 0.60 Myr. Skyline plots reveal that SGM + SPS + Hua lineage showed an increase in *Ne* that occurred ca. 0.2 Myr. Populations of the SEM lineage underwent a gradual

decline in *Ne* around 50,000 years ago, which has continued to the present, whereas, for the NGM lineage a demographic expansion took place around 80,000 years ago (Fig. 4). The GF + Ixt + ChaCal clade experienced a slight reduction in the *Ne* that became more pronounced around 50,000 years ago, followed by a recovery during the late Pleistocene, around 12,000 years ago. In the Colombian Nor + Cen lineage, the demographic expansions are relatively recent, occurring 10,000 years ago. In contrast, the South lineage demographic expansion occurred around 70,000 years ago.

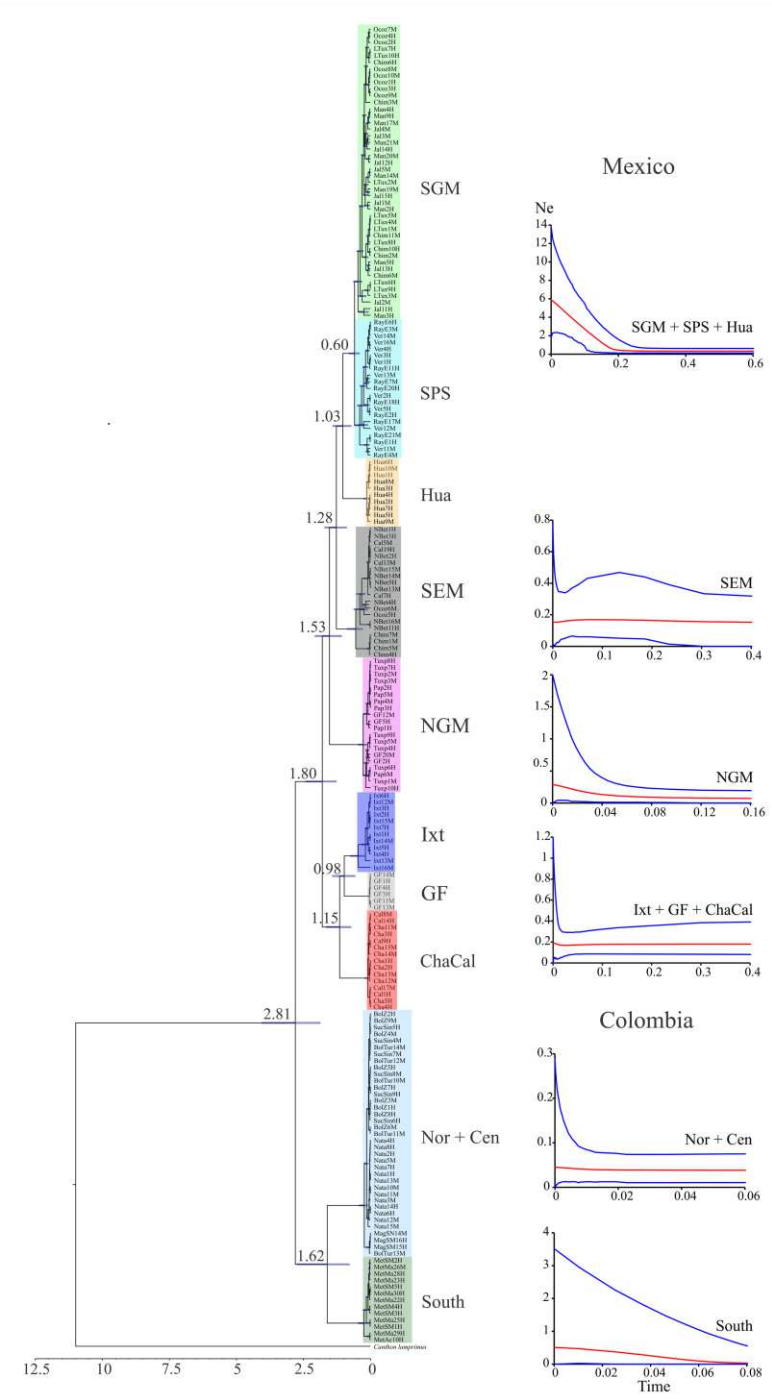


Fig. 4 Time-calibrated phylogeny. Time is given in millions of years. Nodes with posterior probabilities above 0.9 are shown with 95% HPD bars. On the right side, Skyland plots display the historical demographic trends of the major lineages. The red line indicates the median *Ne* trend, while the blue lines represent the 95% confidence limits

Biogeographical scenario

S-DIVA inferred three vicariant and two dispersal events during the evolutionary history of *C. cyanellus* (Fig. 5). The first vicariant event separated the lineages of Colombia and Mexico (node A). Two additional vicariant events occurred: one between the NGM, and several localities south of the Gulf of Mexico and south-southeast of the country (i.e., SGM, Hua, and SEM) (node B); and another between the Ixt and GF clades (node C). One dispersal event was inferred between the Mesoamerican clades (i.e., SEM and SGM + SPS + Hua), and the North American clade NGM (node D) from the remaining areas (i.e., Ixt, ChaCal, and GF). Another dispersal event occurred between GF subclade and the subclades ChaCal and Ixt located north and south of the Trans-Mexican Volcanic Belt, respectively (node E). S-DIVA analysis failed to identify a single ancestral area for the species. Ancestral node reconstruction (Node A) showed ambiguity, with a composite area South America + Mesoamerica being the most frequent, recovered in over 50% of the reconstructions. More recently, the radiation of the species currently distributed in Mexico received a Mesoamerican origin (node D, 50%).

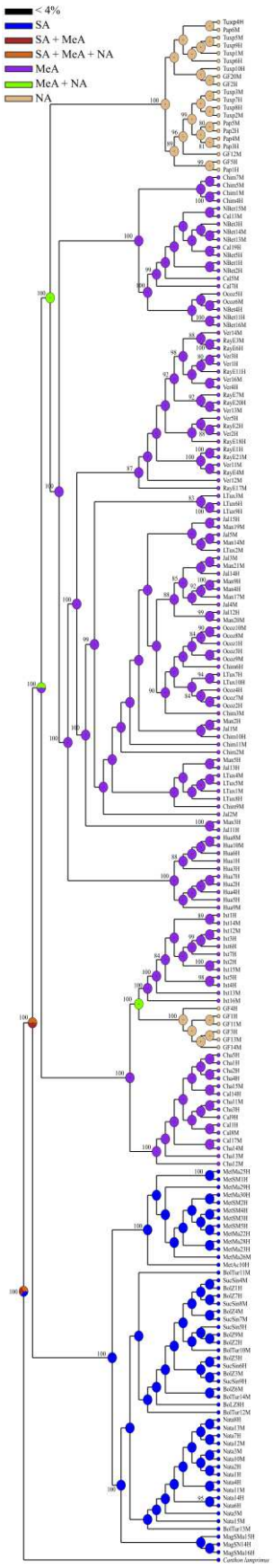

< 4%
SA
SA + MeA
SA + MeA + NA
MeA
MeA + NA
NA

Fig. 5 Biogeographic scenario (dispersal-vicariance) plot based on a condensed tree assembled from 39,996 trees obtained from BEAST. The numbers indicate the marginal probability for each hypothetical ancestral range (only values >80% are shown)

Discussion

The phylogenetic information contained within the mitochondrial and nuclear DNA markers used allows us to understand and reconstruct aspects of the historical demography and diversification of *C. cyanellus*, as well as the possible role that climatic fluctuations and geological events have played. Our results indicate that the genealogical relationship and historical demography of the populations at Colombia and Mexico have been influenced by events such as the uplift of the Andes, the formation of the Isthmus of Panama, and the Quaternary climatic fluctuations. These events have contributed in shaping the current distribution of *C. cyanellus* in the Neotropics, and structuring its genetic diversity. Similar patterns have been documented in other insects in the same biogeographical region (Mendoza-Ramírez et al. 2018; Gergonne et al. 2023; Muñoz-Valencia et al. 2022); nonetheless, their recognition in copro-necrophagous beetles is recent (Nolasco-Soto et al. 2017, 2020, 2023).

Genetic diversity and historical demography

The highest genetic diversity was observed in mitochondrial loci (mtDNA: *COI* and *16S*) and the lowest in nuclear loci (nDNA: *ITS2*) (Table 2). This difference can be attributed to the mutation rate of the mtDNA, estimated to be 5–10 times higher than that of the nDNA (De Mandal et al. 2014). The ANOVA for the genetic diversity parameters showed significant differences between loci and between geographic regions (Table 4, Table S3). The low genetic variation observed in North America and Mesoamerica within the *ITS2* can be explained by the fact that South

American populations have had more time to accumulate mutations (Table 2), and/or by a possible founder event, from South American to North America.

The effect of latitude on genetic diversity also shows differences between mtDNA and nDNA (Fig. S2, Table 3). Mitochondrial markers showed a positive relationship between latitude and genetic diversity (i.e., π and Hd). This allows the detection of geographic gradients of diversity associated with historical and demographic processes (Hewitt 2000; Fonseca et al. 2023; French et al. 2023). In contrast, the *ITS2* due to its recombination and biparental inheritance attenuates the latitudinal signal. In this regard, Fonseca et al. (2023) analyzed mtDNA (i.e., *COI*, *Cytb*) from vertebrates, arachnids, and insects, observing that in insects, an increment in π with respect to latitude does not constitute a general pattern. However, the demographic changes associated with Quaternary glaciations had a lesser impact on tropical species (Fonseca et al. 2023).

Climatic and habitat variations along a latitudinal gradient can influence effective population size and, consequently, the amount of genetic diversity (Fonseca et al. 2023; French et al. 2023). A demographic expansion took place nearly 0.2 Myr ago in populations of *C. cyanellus* from the Gulf of Mexico slope (Jal, Man, LTux), Chiapas (Ocozo), Oaxaca (Chim), and the southern Pacific coast (Hua, Ver, RayE). Such increment in *Ne* coincides with the interglacial Marine Isotope Stage (MIS) 7 (ca. 0.25–0.19 Myr), characterized by a climatic optimum, which may have facilitated habitat expansion, dispersal, and the retention of genetic diversity (Gibbard and West 2000; Berger et al. 2016). Then, local expansions occurred into the slope of the Gulf of Mexico (Tuxp, Pap) ca. 80,000 years ago and into the Eastern Cordillera of the Andes ca. 70,000 years ago. This time matching with the MIS 5 interglacial period (ca. 0.13–0.07 Myr), that was characterized by warm interstadial pulses (Berger et al. 2016). More recent, during the

interglacial period MIS 3 (ca. 0.06–0.03 Myr), forest expansions and contractions occurred due to abrupt cycles of cold and warm weather phases (Gibbard and West 2000; Huber et al. 2006). Throughout this period populations distributed in southeastern Mexico (Nbet, Chim, Cal), at the Pacific coast (Cha, Ixt), and in the Sierra Madre Oriental (GF) showed a slight reduction in the *Ne*. Although, this incipient reduction in southeastern Mexico continues, for the rest of the regions there is a recovery that began ca. 12,000 years ago. Such date corresponds to the end of the Last Glacial Maximum (Lachniet and Vazquez-Selem 2005). Finally, a local population expansion during the Holocene in northern and central Colombia occurred ca. 10,000 years ago, following the glaciations of the Sierra Nevada de Santa Marta, the Eastern Cordillera around Bogotá, the Sierra Nevada del Cocuy, and the Ruiz-Tolima massif at the Central Cordillera (Schubert and Clapperton 1990; Lachniet and Vazquez-Selem 2005). This model of expansions associated with interglacial and climatic refugia has been observed in different taxa in Mexico and in the Andean region (Turchetto-Zolet et al. 2013; Sanabria-Urbán et al. 2025).

Taxonomic implications

The haplotype network and SAMOVA indicate that the lineages within *C. cyanellus* from Mexico and Colombia are genetically and spatially structured. Such structure seems to be the result, at least in part, of historical isolation (Fig. 3). The genealogical pattern recovered is consistent with the genetic structure inferred from the molecular markers used, as well as with recent taxonomic revisions. For Mexico our molecular tree recovers five well-supported clades (i.e., GF, NGM, Ixt, ChaCal, and Hua), plus two other clades that score suboptimal PP values (i.e., SGM + SPS and SEM) (Fig. S6).

Recently, based on external morphological characters (e.g., pronotal puncture, pygidium length and coloration), Rivera-Duarte et al. (2025) have proposed an alternative taxonomic arrangement for *C. cyanellus*. These authors have considered as valid species: 1) *Canthon spinosus* Harold, 1863, distributed from central Veracruz to the Caribbean coast of Honduras, and 2) *Canthon sallei* Harold, 1863, distributed from Central America to southern Mexico. According to these authors, *C. cyanellus violetae* Halffter, 1961, should not be a valid subspecies, and should be a junior synonym of *C. sallei*. Rendering to their distribution, the clade SGM or SEM could be *C. spinosus*, while SPS could belong to *C. sallei*. They recognized *C. cyanellus sensu stricto* as a species distributed from the northern slopes of the Trans-Mexican Volcanic Belt to Texas, USA, which could be either GF or NGM. The lack of specimens from Texas prevents us from inferring the genetic relationship of those populations.

The samples collected in Colombia were recovered in two robust clades (i.e., Nor + Cen and South). The populations encompassed in those clades exhibit polychromatism and high morphological variability (Figs. S1, S6). Nunes (2019) performed a taxonomic revision of *C. cyanellus* and assigned the populations distributed from northern Brazil to northwestern Colombia to *C. triangulatus*. However, our molecular tree suggests that at least two independent lineages have evolved in that area. The sclerite from the internal sac of the aedeagus of the specimens collected at the Natagaima - Tolima locality (Nolasco-Soto et al. 2023) and the material reviewed by Nunes (2019) resembles the morphology described in *C. sallei* for that structure. Therefore, the distribution of this Nor + Cen lineage would cover the Caribbean Sea coasts, as well as the area between the Central and Eastern Andean Mountain ranges. Meanwhile, the Colombian South clade would correspond to *C. triangulatus*.

Both Nunes (2019) and Rivera-Duarte et al. (2025) used morphological characters that had not been considered previously for taxonomic assessment (e.g., Halffter 1961). Our results

agree with the proposal of Rivera-Duarte et al. (2025), who concluded that *C. cyanellus* is a species complex whose speciation process occurred mainly in allopatry during the Pleistocene. It is likely that the complex chromatic variation, as well as the interpopulation morphological variability, has kept multiple historically independent lineages (i.e., species) hidden. The ecosystems where *C. cyanellus* can be found are heterogeneous. More detailed population studies could reveal local adaptations (e.g., physiological, behavioral, and morphological) and thus reinforce recognition of more than one species within the *cyanellus* complex. Indubitably, the taxonomic review of this group is an effort in progress.

General trend in the evolution of *C. cyanellus*

The separation of the Colombian and Mexican populations ca. 2.81 Myr (Fig. 4) coincides with the recent formation of the Isthmus of Panama (O'Dea et al., 2016). This is consistent with a dispersal pattern from South America to North America (Kohlmann and Halffter 1990; Halffter and Morrone 2017). It is possible that the ancestor of *C. cyanellus* was widely distributed in South America during the early Pliocene before the Eastern Cordillera of the Andes rose to become a geographic barrier separating the Colombian clades ca. 1.62 Myr. Paleobotanical data suggests a rapid uplift of the Eastern Cordillera of the Andes ca. 2–5 Myr (Gregory-Wodzicki 2000). A similar roll of the Panamanian land bridge on the dispersion process has been proposed for ants (Mendoza-Ramírez et al. 2018) and fruit flies (Freilij et al. 2024). However, the date of the final closure of the Isthmus of Panama is still under debate (Montes et al. 2015; Bacon et al. 2015; O'Dea et al. 2016). Furthermore, there is evidence suggesting that the dispersal of different taxa across the Isthmus of Panama occurred before 3 Myr (beetles: Huang 2016; ants: Winston et al. 2017).

The Andes constitute an effective biogeographic barrier for numerous taxa and an important area of speciation for arthropods (Muñoz-Valencia et al. 2022; Gergonne et al. 2023; Salgado-Roa et al. 2024). The altitudinal distribution of *C. cyanellus* ranges from 0–1500 m above sea level (Solís and Kohlmann 2002). Therefore, its dispersal across the Andean Mountain range seems improbable. Similar altitudinal limitations have been documented in other coprophagous beetles (Larsen 2012). Nonetheles, the local mobility of *C. cyanellus* suggests a potential for geographic expansion (Arellano et al. 2008). We should not rule out the possibility that Colombian lineages may coexist in some areas, such as the lowlands connecting eastern Venezuela with northern Colombia, surrounding the northern flank of the Andes, where specimens have been collected (Lozano et al. 2024). A similar dispersal scenario has been proposed for the invasive beetle *Digitonthophagus gazella* (Fabricius, 1787) upon its entry into Colombia (Noriega et al. 2017) or for termites of the genus *Embiratermes*, indicating the potential of this pathway for the dispersal of insects confronting altitudinal limitations (Gergonne et al. 2023).

The ambiguity in reconstructing the ancestral range, which suggests an ancestor widely distributed across South and Mesoamerica, stems from the clear genetic differentiation between populations from both geographic areas (Fig. 5). According to Padilla and Halffter (2007), the Scarabaeinae fauna, particularly Deltochilini, shows biogeographic affinity with taxa from Costa Rica and Colombia. This is based on the historical, geological, and ecological processes that influenced the formation of Mesoamerican tropical dry forests. These authors postulate that the origin and current distribution of tropical dry forests occurred during the Pleistocene, which facilitated multiple expansion and speciation events from South America. The future incorporation of biological material from Central America will be crucial to testing this hypothesis and refining the biogeographic history of *C. cyanellus*.

The phylogeographic analysis of *C. cyanellus* suggests that its current demography, genetic structure, and distribution are the result of the interaction between geological history and Quaternary climatic changes in the Neotropics. Our results suggest synchronized demographic expansions among different lineages during interglacial or interstadial periods. Currently, these demographic expansions may be related to changes in landscape composition due to the intensification of tropical deforestation and agriculture, which have facilitated their invasion into grasslands (Arellano et al. 2008; Salomão et al. 2018). While the divergence between the Colombian and Mexican populations (~2.81 Myr) coincides with the early formation of the Isthmus of Panama, further refinement of the biogeographic history is required in future studies that include Central American populations.

Data accessibility

Supplementary information is available online.

Acknowledgments

We thank Carlos Taboada, Charles Andrés Zapata, Santiago Rodríguez, and Candelaria Ortega for their invaluable assistance with sample collection in Colombia. Claudio Mota Vargas kindly contributed Figure 2. We are also grateful to José Daniel Rivera for donating the *Canthon cyanellus* specimens from Ocozocoautla, Chiapas, and to Cristina Bárcenas Pazos for her technical assistance in sequencing the samples from Chiapas.

Author contribution

Janet Nolasco-Soto: data curation, formal analysis, methodology, writing-original draft, writing-review and editing. Jorge González-Astorga, Mario E. Favila, and Alejandro Espinosa de los Monteros: conceptualization, formal analysis, methodology, resources, writing-review & editing; Jorge Ari Noriega: data curation, writing-review & editing.

Funding

No funds, grants, or other support were received.

Data Availability

The *COI*, *16S*, and *ITS2* marker sequence data that support the findings of this study are openly available from NCBI GenBank at https://www.ncbi.nlm.nih.gov. Additional information can be found in the supplementary material.

Declarations

Ethical Approval: Not applicable.

Competing interests: We declare we have no competing interests.

References

Arellano L, León-Cortés J, Ovaskainen O (2008) Patterns of abundance and movement in relation to landscape structure: a study of a common scarab (*Canthon cyanellus cyanellus*) in Southern Mexico. Landscape Ecol 23:69–78. https://doi.org/10.1007/s10980-007-9165-8

Arias CF, Salazar C, Rosales C, Kronforst MR, Linares M, Bermingham E, McMillan WO (2014) Phylogeography of *Heliconius cydno* and its closest relatives: disentangling their origin and diversification. Mol Ecol 23:4137–4152. https://doi.org/10.1111/mec.12844

Bacon CD, Molnar P, Antonelli A, Crawford AJ, Montes C, Vallejo-Pareja MC (2016) Quaternary glaciation and the Great American Biotic Interchange. Geology 44:375–378. https://doi.org/10.1130/G37624.1

Bacon CD, Silvestro D, Jaramillo C, Smith BT, Chakrabarty P, Antonelli A (2015) Biological evidence supports an early and complex emergence of the Isthmus of Panama. Proc Natl Acad Sci 112:6110-6115. https://doi.org/10.1073/pnas.1423853112

Berger A, Crucifix M, Hodell DA, Mangili C, McManus JF, Otto-Bliesner B, Pol K, Raynaud D, Skinner LC, Tzedakis PC, Wolff EW, Yin QZ, Abe-Ouchi A, Barbante C, Brovkin V, Cach I, Capron E, Ferretti P, Ganopolski A, Grimalt JO, Hönisch B, Kawamura K, Landais A, Margari V, Martrat B, Masson-Delmotte V, Mokeddem Z, Parrenin F, Prokopenko AA, Rashid H, Schulz M, Vazquez Riveiro N (2016) Interglacials of the last 800,000 years. Rev Geophys 54:162–219. https://doi:10.1002/2015rg000482. hal-03245836

Caccone A, Amato GD, Powell JR (1988) Rates and patterns of scnDNA and mtDNA divergence within the *Drosophila melanogaster* Subgroup. Genetics 118:671–685. https://doi.org/10.1093/genetics/118.4.671

Capra L, Bernal JP, Carrasco-Núñez G, Roverato M (2013) Climatic fluctuations as a significant contributing factor for volcanic collapses. Glob Planet Change 100:194–203. https://doi.org/10.1016/j.gloplacha.2012.10.017

Chani-Posse MR, Rodríguez-Melgarejo ME (2024) Origin and early diversification of a high Andean rove-beetle clade: *Corisantis* gen. nov., phylogeny, and historical biogeography. J Comp Zool 313:395–416. https://doi.org/10.1016/j.jcz.2024.11.002

Cody S, Richardson JE, Rull V, Ellis C, Pennington RT (2010) The Great American Biotic Interchange revisited. Ecography 33:326–332. https://doi.org/10.1111/j.1600-0587.2010.06327.x

Cupello M, Ribeiro-Costa CS, Vaz-de-Mello F (2021) The evolution of *Bolbites onitoides* (Coleoptera: Scarabaeidae: Phanaeini): its phylogenetic significance, geographical polychromatism, and the subspecies problem. Zool J Linn Soc XX:1–62. https://doi.org/10.1093/zoolinnean/zlab015

Cupello M, Silva FAB, Vaz-de-Mello FZ (2023) The taxonomic revolution of New World dung beetles (Coleoptera: Scarabaeidae: Scarabaeinae). Front Ecol Evol 11:1168754. https://doi.org/10.3389/fevo.2023.1168754

Darriba D, Taboada GL, Doallo R, Posada D (2012) jModelTest 2: more models, new heuristics and parallel computing. Nat Methods 9:772. https://doi.org/10.1038/nmeth.2109

De Mandal S, Chhakchhuak L, Gurusubramanian G, Kumar NS (2014) Mitochondrial markers for identification and phylogenetic studies in insects – A review. DNA Barcodes 2:1–9. https://doi.org/10.2478/dna-2014-0001

Drummond AJ, Suchard MA, Xie D, Rambaut A (2012) Bayesian phylogenetics with BEAUti and BEAST 1.7. Mol Biol Evol 29:1969–1973. https://doi.org/10.1093/molbev/mss075

Dupanloup IS, Schneider S, Excoffier L (2002) A simulated annealing approach to define the genetic structure of populations. Mol Ecol 11:2571–2581. https://doi.org/10.1046/j.1365-294X.2002.01650.x

Excoffier L, Lischer HEL (2010) Arlequin suite ver 3.5: a new series of programs to perform population genetics analyses under Linux and Windows. Mol Ecol Resour 10:564–567. https://doi.org/10.1111/j.1755-0998.2010.02847.x

Excoffier L, Smouse P, Quattro JM (1992) Analysis of molecular variance inferred from metric distances among DNA restriction data. Genetics 131:479–491. https://doi.org/10.1093/genetics/131.2.479

Ferrari L, Tagami T, Eguchi M, Orozco-Esquivel MT, Petrone CM, Jacobo-Albarrán J, López-Martínez M (2005) Geology, geochronology and tectonic setting of late Cenozoic volcanism along the Southwestern Gulf of Mexico: the Eastern Alkaline Province revisited. J Vol Geothe Res 146:284–306. https://doi.org/10.1016/j.jvolgeores.2005.02.004

Fonseca EM, Pelletier TA, Decker SK, Parsons DJ, Carstens BC (2023) Pleistocene glaciations caused the latitudinal gradient of within-species genetic diversity. Evol Lett 5:331–338. https://doi.org/10.1093/evlett/qrad030

Freilij D, Vilardi JC, Gómez-Cendra P (2024) Rapid cryptic divergence of the *Anastrepha fraterculus* complex in the Late Pleistocene: a phylogeographical–ecological approach. Biol J Linn Soc 142:21–37. https://doi.org/10.1093/biolinnean/blad116

French CM, Bertola LD, Carnaval AC, Economo EP., Kass JM., Lohman DJ, Marske KA, Meier R, Overcast I, Rominger AJ, Staniczenko PPA, Hickerson MJ (2023) Global determinants of insect mitochondrial genetic diversity. Nat Commun 14:5276. https://doi.org/10.1038/s41467-023-40936-0

Gergonne D, Fougeyrollas R, Poteaux C, Roisin Y,·Armbrecht I, Šobotník J, Valladares Romero CS, Berthier JM, Sillam-Dusses D, Roy V (2023) The phylogeography of some soil-feeding termites shaped by the Andes. Org Divers Evol 23:381–394. https://doi.org/10.1007/s13127-022-00594-4

Gibbard PL, West RG (2000) Quaternary chronostratigraphy: the nomenclature of terrestrial sequences. Boreas 29:329–336. https://doi.org/10.1111/j.1502-3885.2000.tb01214.x

Gregory-Wodzicki KM (2000) Uplift history of the Central and Northern Andes: A review. Geol Soc Am Bull 112:1091–1105. https://doi.org/10.1130/0016-7606(2000)112<1091:UHOTCA>2.0.CO;2

Gunter NL, Weir TA, Slipinksi A, Bocak L, Cameron SL (2016) If dung beetles (Scarabaeidae: Scarabaeinae) arose in association with dinosaurs, did they also suffer a mass co-extinction at the K-Pg boundary? PLoS ONE 11:e0153570. https://doi.org/10.1371/journal.pone.0153570

Halffter G (1976) Distribución de los insectos en la Zona de Transición Mexicana. Folia Entomol Mex 35:1–64.

Halffter G (1974) Elements anciens de l'entomofaune neotropicale: ses implications biog_eographiques. Quaest Entomol 10:223–262.

Halffter G (1964) La entomofauna americana, ideas acerca de su origen y distribución. Folia Entomol Mex 6:1–108.

Halffter G (1961) Monografía de las especies norteamericanas del género *Canthon* Hoffsg. (Coleop., Scarab.). Ciencia 20:225–320.

Halffter G, Martínez A (1977) Revisión monográfica de los Canthonina americanos. Parte IV. Clave para géneros y subgéneros. Folia Entomol Mex 38:29–107.

Halffter G, Morrone JJ (2017) An analytical review of Halffter's Mexican transition zone and its relevance for evolutionary biogeography, ecology, and biogeographical regionalization. Zootaxa 4226:1–46. https://doi.org/10.11646/zootaxa.4226.1.1

Hewitt G (2000) The genetic legacy of the Quaternary ice ages. Nature 405:907–913. https://doi.org/10.1038/35016000

Hoorn C, Wesselingh FP, ter Steege H, Bermudez MA, Mora A, Sevink J, Sanmartín I, Sanchez-Meseguer A, Anderson CL, Figueiredo JP, Jaramillo C, Riff D, Negri FR, Hooghiemstra H, Lundberg J, Stadler T, Särkinen T, Antonelli A (2010) Amazonia through time: Andean uplift, climate change, landscape evolution, and biodiversity. Science 330:927–931. https://doi.org/10.1126/science.1194585

Huang JP (2016) The great American biotic interchange and diversification history in *Dynastes* beetles (Scarabaeidae; Dynastinae). Zool J Linn Soc 178:88–96. https://doi.org/10.1111/zoj.12393

Huber C, Leuenberger M, Spahni R, Flückiger J, Schwander J, Stocker TF, Jouzel J (2006) Isotope calibrated Greenland temperature record over Marine Isotope Stage 3 and its relation to CH4. Earth Planet Sci Lett 243:504–519. https://doi.org/10.1016/j.epsl.2006.01.002

Kohlmann B, Halffter G (1990) Reconstruction of a specific example of insect invasion waves: the cladistic analysis of *Canthon* (Coleoptera: Scarabaeidae) and related genera in North Amer*ica.* Quaest Entomol 26:1–28.

Kumar S, Stecher G, Li M, Knyaz C, Tamura K (2018) MEGA X: Molecular evolutionary genetics analysis across computing platforms. Mol Biol Evol 35:1547–1549. https://doi.org/10.1093/molbev/msy096

Lachniet MS, Vazquez-Selem L (2005) Last Glacial Maximum equilibrium line altitudes in the circum-Caribbean (Mexico, Guatemala, Costa Rica, Colombia, and Venezuela). Quat Int 138:129–144. https://doi.org/10.1016/j.quaint.2005.02.010

Larsen TH (2012) Upslope range shifts of Andean dung beetles in response to deforestation: compounding and confounding effects of microclimatic change. Biotropica 44:82–89. https://doi.org/10.1111/j.1744-7429.2011.00768.x

Leigh JW, Bryant D (2015) PopART: full-feature software for haplotype network construction. Methods Ecol Evol 6:1110–1116. https://doi.org/10.1111/2041-210X.12410

Lozano de la Rosa C, Cupello M, Vaz-de-Mello FZ (2024) The dung beetles of Venezuela (Coleoptera: Scarabaeidae: Scarabaeinae): catalogue and updated distribution. Eur J Taxon 959:1–272. https://doi.org/10.5852/ejt.2024.959.2677

Maldaner ME, Vaz-de-Mello FZ, Takiya DM, Ferreira DC (2019) Genetic and chromatic variation of *Coprophanaeus* (*Megaphanaeus*) *ensifer*. Zool Anz 283:150–160. https://doi.org/10.1016/j.jcz.2019.09.001

Martínez A (1988) Algunos Scarabaeinae neotropicales nuevos o poco conocidos. Rev Cient UNET 2:85–90.

Mendoza-Ramírez M, Gutiérrez-Rodríguez J, Poteaux C, Ornelas-García P, Zaldívar-Riverón A (2018) Late Pleistocene genetic diversification and demographic expansion in *Neoponera villosa* (Ponerinae). Mitochondrial DNA A 30:296–306. https://doi.org/10.1080/24701394.2018.1493469

Miller MA, Pfeiffer W, Schwartz T (2010) Creating the CIPRES Science Gateway for inference of large phylogenetic trees. 2010 Gateway Computing Environments Workshop (GCE), New Orleans, LA, USA, pp. 1–8. https://doi.org/10.1109/GCE.2010.5676129

Moctezuma V, Sánchez-Huerta JL, Espinosa de los Monteros A, Nolasco-Soto J, Gonzalo H (2025) Description of Three New Species of the *Canthon indigaceus* Species Group (Coleoptera: Scarabaeidae: Scarabaeinae). Taxonomy 5:26. https://doi.org/10.3390/taxonomy5020026

Montes C, Cardona A, Jaramillo C, Pardo A, Silva JC, Valencia V, Ayala C, Pérez-Angel LC, Rodríguez-Parra LA, Ramírez JC, Niño H (2015) Middle Miocene closure of the Central American seaway. Science 348:226–228. https://doi.org/10.1126/science.aaa2815

Morrone JJ (2020) The biotic assembly of the Mexican Transition Zone. In: Morrone JJ (ed) The Mexican Transition Zone. Springer, Cham. pp. 157–180. https://doi.org/10.1007/978-3-030-47917-6_1

Muñoz-Valencia V, Vélez-Martínez GA, Montoya-Lerma J, Díaz F (2022) Role of the Andean uplift as an asymmetrical barrier to gene flow in the neotropical leaf-cutting ant *Atta cephalotes*. Biotropica 54:191–204. https://doi.org/10.1111/btp.13050

Mush DR (2002) Evidence for the timing and duration of the last interglacial period from high-precision Uranium-Series Ages of corals on tectonically stable coastlines. Quaternary Res 58:36–40. https://doi.org/10.1006/qres.2002.2339

Nei M, Li WH (1979) Mathematical model for studying genetic variation in terms of restriction endonucleases. Proc Natl Acad Sci USA 76:5269–5273. https://doi.org/10.1073/pnas.76.10.5269

Nolasco-Soto J, Favila ME, Espinosa de los Monteros A, González-Astorga J, Halffter G, Valdez-Carrasco J, Ari Noriega J, Galante E (2020) Variations in genetic structure and male genitalia suggest recent lineage diversification in the *Canthon cyanellus* complex. Biol J Linn Soc 131:505–520. https://doi.org/10.1093/biolinnean/blaa131

Nolasco-Soto J, González-Astorga J, Espinosa de los Monteros A, Galante-Patiño E, Favila ME (2017) Phylogeographic structure of *Canthon cyanellus* in the Mexican Transition Zone. Mol Phylogenet Evol 109:180–190. https://doi.org/10.1016/j.ympev.2017.01.004

Nolasco-Soto J, González-Astorga J, Espinosa de los Monteros A, Favila ME (2023) Evolutionary history and diversity in the ball roller beetle *Canthon cyanellus*. Front Ecol Evol 10:1066439. https://doi.org/10.3389/fevo.2022.1066439

Noriega JA, Delgado O, Blanco JI, Gamez J, Clavijo J (2017) Introduction, establishment, and invasion of *Digitonthophagus gazella* (Fabricius, 1787) (Coleoptera: Scarabaeinae) in the Savannas of Venezuela and Colombia. Natural Resources 8:370-381. https://saber.ucv.ve/handle/10872/23643

Nunes LGOA (2019) Revisão taxonômica e definição de alguns grupos de espécies do gênero Canthon Hoffmannsegg (Coleoptera: Scarabaeidae: Scarabaeinae: Deltochilini). Doctoral Thesis. Universidade Federal de Pernambuco.

O'Dea A, Lessios HA, Coates AG, Eytan RI, Restrepo-Moreno SA, Cione AL, Collins LS, de Queiroz A, Farris DW, Norris RD, Stallard RF, Woodburne MO, Aguilera O, Aubry MP, Berggren WA, Budd AF, Cozzuol MA, Coppard SE, Duque-Caro H, Finnegan S, Gasparini GM, Grossman EL, Johnson KG, Keigwin LD, Knowlton N, Leigh EG, Leonard Pingel JS, Marko PB, Pyenson ND, Rachello-Dolmen PG, Soibelzon E, Soibelzon L, Todd JA, Vermeij GJ, Jackson JBC (2016) Formation of the Isthmus of Panama. Science Advances 2:e1600883. https://doi.org/10.1126/sciadv.1600883

Padilla-Gil DN, Halffter G (2007) Biogeography of Canthonini in Mesoamerica and Colombia. Acta Zool Mex (n.s.) 23:73–108.

Papadopoulou A, Anastasiou I, Vogler AP (2010) Revisiting the insect mitochondrial molecular clock. Mol Biol Evol 27:1659–1672. https://doi.org/10.1093/molbev/msq051

Rambaut A (2008) FigTree v.1.3.1. Institute of Evolutionary Biology, University of Edinburgh. http://tree.bio.ed.ac.uk/software/figtree/

Rambaut A, Drummond AJ, Xie D, Baele G, Suchard MA (2018) Posterior summarization in Bayesian phylogenetics using Tracer 1.7. Syst Biol 67:901–904. https://doi.org/10.1093/sysbio/syy032

Reyes JA, Espinosa de los Monteros A, Santiago-Jiménez QJ (2023) Phylogeography of *Falagonia mexicana* Sharp, 1883 (Coleoptera, Staphylinidae, Aleocharinae). ZooKeys 1156:107–131. https://doi.org/10.3897/zookeys.1156.84943

Rivera-Duarte JD, Salomão RP, Solís A, Michel M, Matamoros MI, Kohlmann B (2025) The Bolboceratidae, Geotrupidae (Coleoptera, Scarabaeoidea), and Scarabaeinae (Coleoptera, Scarabaeoidea, Scarabaeidae) fauna of Honduras: Taxonomy and distribution. ZooKeys 1255:127–206. https://doi.org/10.3897/zookeys.1255.150586

Ronquist F, Teslenko M, van der Mark P, Ayres DL, Darling A, Höhna S, Larget B, Liu L, Suchard MA, Huelsenbeck JP (2012) MrBayes 3.2: Efficient Bayesian phylogenetic inference and model choice across a large model space. Syst Biol 61:539–542. https://doi.org/10.1093/sysbio/sys029

Rozas J, Ferrer-Mata A, Sánchez-DelBarrio JC, Guirao-Rico S, Librado P, Ramos-Onsins SE, Sánchez-Gracia A (2017) DnaSP 6: DNA sequence polymorphism analysis of large datasets. Mol Biol Evol 34:3299–3302. https://doi.org/10.1093/molbev/msx248

Rull V (2011) Neotropical biodiversity: timing and potential drivers. Trends Ecol & Evol 26: 508–513. https://doi.org/10.1016/j.tree.2011.05.011

Salomão PR, González-Tokman D, Dáttilo W, López-Acosta JC, Favila ME (2018) Landscape structure and composition define the body condition of dung beetles (Coleoptera: Scarabaeinae) in a fragmented tropical rainforest. Ecol Indic 88:144–151. https://doi.org/10.1016/j.ecolind.2018.01.033

Salgado-Roa FS, Pardo-Díaz C, Rueda-MN, Cisneros-Heredia DF, Lasso E, Salazar C (2024) The Andes as a semi-permeable geographical barrier: genetic connectivity between structured populations in a widespread spider. Mol Ecol 33:e17361. https://doi.org/10.1111/mec.17361

Sanabria-Urbán S, Torres-Miranda A, Prieto-Torres DA, Oyama K, Cueva del Castillo R (2025) Pleistocene Climate Changes and Lineage Diversification of *Sphenarium* Grasshoppers (Orthoptera: Pyrgomorphidae). Ecol Evol 15:e72209. https://doi.org/10.1002/ece3.72209

Schoolmeesters P (2026) World Scarabaeidae Database (version 2026-04-03). In: Bánki O, Roskov Y, Döring M, et al. *Catalogue of Life (Version 2026-04-10)*. Catalogue of Life, Amsterdam. https://www.checklistbank.org/dataset/309120/taxon/6278C

Schubert C, Clapperton CM (1990) Quaternary glaciations in the northern Andes (Venezuela, Colombia and Ecuador). Quat Sci Rev 9:123–135. https://doi.org/10.1016/0277-3791(90)90014-2

Schmidt A (1922) 1) Bestimmungstabelle den bekannten *Canthon*-Arten. 2) Verbreitungsgebiete der *Canthon*-Arten. 3) Neubeschreinbungen von *Canthon*, Saprosites, Mendidius, Euparia und Ataenius. Arch Naturg 88:Abt. A: 61–103.

Smith BT, Amei A, Klicka J (2012) Evaluating the role of contracting and expanding rainforest cycles and speciation across the Isthmus of Panama. Proc R Soc B 279:3520–3526. https://doi.org/10.1098/rspb.2012.0706

Solís A, Kohlmann B (2002) El género *Canthon* en Costa Rica. G Ital Entomol 10:1–68.

Turchetto-Zolet AC, Pinheiro F, Salgueiro F, Palma-Silva C (2013) Phylogeographical patterns shed light on evolutionary process in South America. Mol Ecol 22:1193–1213. https://doi.org/10.1111/mec.12164

Vaz-de-Mello FZ, Cupello M (2018) The type specimens of South American dung beetles. Part I: on the species described in the genus *Canthon* Hoffmannsegg, 1817 by the German entomologist Adolf Schmidt (1856-1923): (Coleoptera, Scarabaeidae, Scarabaeinae). Spixiana 41:33–76.

Winston ME, Kronauer DJC, Moreau CS (2017) Central American colonization and speciation in army ants. Mol Ecol 26:859–870. https://doi.org/10.1111/mec.13846

Yu Y, Blair C, He XJ (2020) RASP 4: Ancestral state reconstruction for multiple genes. Mol Biol Evol 37:604–606. https://doi.org/10.1093/molbev/msz257

Supplementary figures

Fig. S1 Body colour variation in Colombian populations. Photos at the top show individuals collected in northern and central Colombia (i.e., Nor + Cen clade). Photos at the bottom show individuals collected east of the Eastern Cordillera of the Andes (i.e., South clade).

Fig. S2 Global linear regression between latitude *vs.* π and latitude *vs.* Hd by locus.

Fig. S3 Haplotype networks for *ITS2* nuclear gene. Roman numerals indicate the respective haplogroups and the size of the pie chart is proportional to haplotype frequency. Mutational changes are indicated in parentheses.

Fig. S4 Haplotype networks for *16S* rRNA mitochondrial gene.

Fig. S5 Haplotype networks for *COI* mitochondrial gene.

Fig. S6 Bayesian consensus tree. Numbers indicate Bayesian posterior probabilities. SGM (Southern Gulf of Mexico: Jalcomulco, Los Tuxtlas, La Mancha, Los Chimalapas, and Ocozocoautla); SPS (Southern Pacific Slope: El Vergel and Raymundo Enríquez); Hua (Huatulco); Ixt (Ixtapa); GF (Gómez Farias); ChaCal (Chamela and Calakmul); NGM (Northern Gulf of Mexico: Papantla, GF, and Tuxpan); SEM (South-Eastern Mexico: Nueva Betania, Calakmul, Los Chimalapas, and Ocozocoautla); Nor + Cen (Zambrano, Turbaco, Sierra Nevada, Santa Marta, Sincelejo, Natagaima); South (La Macarena, Acacias, and San Martín).

Supplementary Files

This is a list of supplementary files associated with this preprint. Click to download.

- Fig.S1.tif
- Fig.S2.tif
- Fig.S3.tif
- Fig.S4.tif
- Fig.S5.tif
- FigS6.tif
- TablesSupportingInformation.docx